Nanowires

International Edition: DOI: 10.1002/anie.201508704
German Edition: DOI: 10.1002/ange.201508704

Solution-Liquid-Solid Synthesis of Hexagonal Nickel Selenide Nanowire Arrays with a Nonmetal Catalyst

Kun Xu[+], Hui Ding[+], Kaicheng Jia, Xiuli Lu, Pengzuo Chen, Tianpei Zhou, Han Cheng, Si Liu, Changzheng Wu, and Yi Xie*

Abstract: *Inorganic nanowire arrays hold great promise for next-generation energy storage and conversion devices. Understanding the growth mechanism of nanowire arrays is of considerable interest for expanding the range of applications. Herein, we report the solution-liquid-solid (SLS) synthesis of hexagonal nickel selenide nanowires by using a nonmetal molecular crystal (selenium) as catalyst, which successfully brings SLS into the realm of conventional low-temperature solution synthesis. As a proof-of-concept application, the NiSe nanowire array was used as a catalyst for electrochemical water oxidation. This approach offers a new possibility to design arrays of inorganic nanowires.*

One-dimensional inorganic nanowires have attracted tremendous interest as a result of their unique physical and chemical properties arising from the quantum confinement effect, and show promising applications in catalysis and electronics, as well as for energy storage and conversion.[1–4] In particular, inorganic nanowire arrays are highly desirable for energy storage and conversion devices because they can provide enough open space to ensure the efficient use of active materials.[5,6] Nanowire arrays could also facilitate the penetration of the electrolyte and reduce the ionic diffusion path.[7] For example, arrays of metal oxide nanowires have been shown to exhibit extremely high electrocatalytic activity in the oxidation of water.[8] Conducting arrays of polymer nanowires have proven to be an ideal electrode material for high-performance supercapacitors.[9] However, as the growth mechanism of most of the nanowire arrays is still unclear, their further applications in diverse fields are limited.

Vapor-liquid-solid (VLS) and solution-liquid-solid (SLS) methods have been widely used to synthesis inorganic nanowires.[10–12] In a typical VLS growth process, the vapor-phase precursor reacts in a liquid droplet of the catalyst, before the solid product crystallizes and is finally deposited to grow nanowires.[13] Analogous to the VLS process, SLS also needs catalyst droplets to catalyze the growth of nanowires, but it is a low-temperature route ($< 300\,^{\circ}C$) and cost-effective, which opens up a new possibility to control the growth of nanowires in solution.[14,15] In SLS processes, low-melting-point metals, such as In, Sn, or Bi, are usually applied as liquid catalysts to grow nanowires, the shape and size of which influence the diameter of the grown nanowires.[16–18] However, after the SLS growth process, etching treatment is required to remove the metal catalysts so that pure nanowires can be obtained. The introduction and removal of metal catalysts make the synthesis of nanowires cumbersome.

Compared with metals such as In, Sn, and Bi, molecular crystals of nonmetals, including S, Se, and I_2, usually have weaker interaction forces between molecules, thereby resulting in lower melting points. The use of a nonmetallic molecular crystal as a catalyst for SLS growth would offer more advantages: the lowering of the melting point could enable SLS nanowires to grow in a wide variety of solutions, and it is more convenient to remove the capping catalyst after the SLS process. Moreover, a nonmetal molecular crystal is cheaper than a metal-based catalyst. In this regard, we wondered whether a nonmetal molecular catalyst could assist the growth of nanowires. To the best of our knowledge, however, most of studies consider a metal-assisted SLS mechanism. Herein, we report that an array of hexagonal nickel selenide nanowires can be synthesized by SLS using a nonmetal molecular crystal as a catalyst, and thus bring SLS into the realm of conventional low-temperature solution synthesis. In our case, a Se crystal in solution serves as both the growth catalyst and Se source for the growth of NiSe nanowires. As a proof-of-concept application, the array of NiSe nanowires was used as an efficient electrocatalyst for the oxygen evolution reaction (OER). This study not only provides a new approach for designing inorganic nanowire arrays, but also provides insight into the SLS synthesis of inorganic nanowires by using a nonmetal catalyst.

In our case, the array of NiSe nanowires grown on a Ni foam was achieved by a conventional low-temperature synthesis method in solution, whereby a bare Ni foam was treated with Se powder in a solution of $NaBH_4$. X-ray diffraction (XRD) was first performed to study the phase and purity of the obtained sample. As shown in Figure 1 a, the XRD pattern could be well indexed to pure hexagonal NiSe (JCPDS Card No. 02-0892; space group: $P63/mmc$; $a = b = 3.66$ Å; $c = 5.33$ Å), thus suggesting that the obtained NiSe nanowires were of high purity. The two strong peaks at 44.5° and 52° arise from the Ni foam substrate (Figure S3). Scanning electron microscopy (SEM) and transmission electron microscopy (TEM) studies were conducted to unravel the morphology of the NiSe samples. The SEM images of the

[*] Dr. K. Xu,[+] H. Ding,[+] K. C. Jia, X. L. Lu, P. Z. Chen, T. P. Zhou, H. Cheng, S. Liu, Prof. C. Z. Wu, Prof. Y. Xie
Hefei National Laboratory for Physical Science at the Microscale
iChEM (Collaborative Innovation Center of Chemistry for Energy Materials), Hefei Science Center (CAS), and CAS Key Laboratory of Mechanical Behavior and Design of Materials
University of Science & Technology of China
Hefei, Anhui 230026 (P. R. China)
E-mail: czwu@ustc.edu.cn

[+] These authors contributed equally to this work.

Supporting information for this article is available on the WWW under http://dx.doi.org/10.1002/anie.201508704.

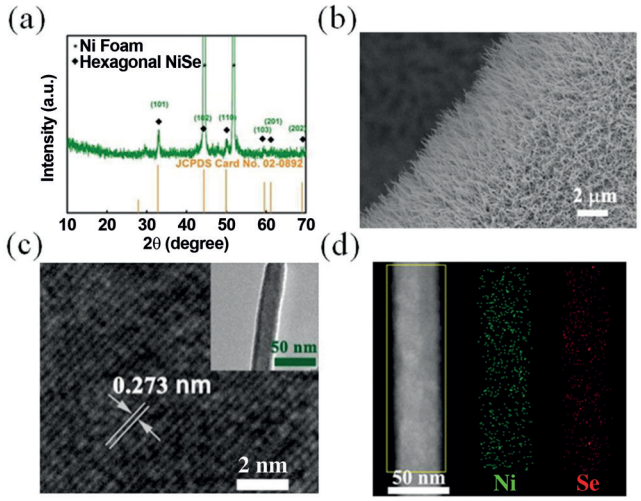

Figure 1. a) XRD pattern of NiSe nanowires grown on an Ni foam. b) SEM image of the NiSe nanowire array. c) HRTEM image of an NiSe nanowire; inset: TEM image. d) HAADF-STEM image and corresponding elemental mappings of the NiSe nanowire.

samples demonstrated the structure of the nanowire arrays (Figure 1b and Figure S4). The TEM image presented in Figure 1c (inset) also reveals that the obtained samples were nanowires. Furthermore, high-resolution transmission electron microscopy (HRTEM) and energy-dispersive X-ray (EDX) studies were carried out to investigate the microscopic structure and elemental compositions of the obtained nanowires. The HRTEM image of an NiSe nanowire exhibited a distinct lattice fringe of 0.273 nm, which agreed well with the (101) lattice plane of hexagonal NiSe (Figure 1c). The EDX results further confirmed that only Se and Ni elements exist in the NiSe nanowires (see Figure S5), which also proves that our obtained NiSe nanowires are of high quality. HAADF-STEM studies and the corresponding elemental mappings were also carried out to examine the elemental distribution in the nanowires (Figure 1d). Both Ni and Se were found to be homogeneously distributed within the NiSe nanowires. The above results clearly demonstrated that hexagonal NiSe nanowires were successfully grown on the Ni foam.

Time-dependent morphology experiments were carried out by SEM to understand the formation mechanism of the NiSe nanowires. The original Ni foam substrate has a clean surface (Figure S2), thus offering the opportunity to grow nanowires on its surface. In an initial stage, some droplets were formed and randomly deposited on the Ni foam substrate (Figure 2a). As the reaction proceeded, nanowires started to form between the Ni foam substrate and the Se droplets (Figure 2b,c). At the end of the reaction, the Ni foam surface was covered with a dense array of long nanowires. Tiny droplets (particle) were still readily observed at the tips of most nanowires, thus suggesting that the mechanism of nanowire growth follows the SLS approach (Figure 2d). The TEM images show that as-formed spherical particles were located at the tips of the nanowires during the SLS reaction (Figure 2f,g). It is noteworthy that the tiny particles disappear after heat treatment and a red substance, which may be selenium, appears on the quartz tube. To verify whether the droplet is selenium, HAADF-STEM and corresponding elemental mappings were utilized. Elemental mapping of an NiSe nanowire with a tiny particle at its tip (Figure 2h) reveals that the tip was rich in Se, thus giving evidence that the particles were selenium. Thus, the growth mechanism of the array of NiSe nanowires was established as following a SLS growth mechanism with a nonmetal Se catalyst.

As a proof-of-concept application, the NiSe nanowires/Ni foam were directly used as an electrocatalyst for the OER.

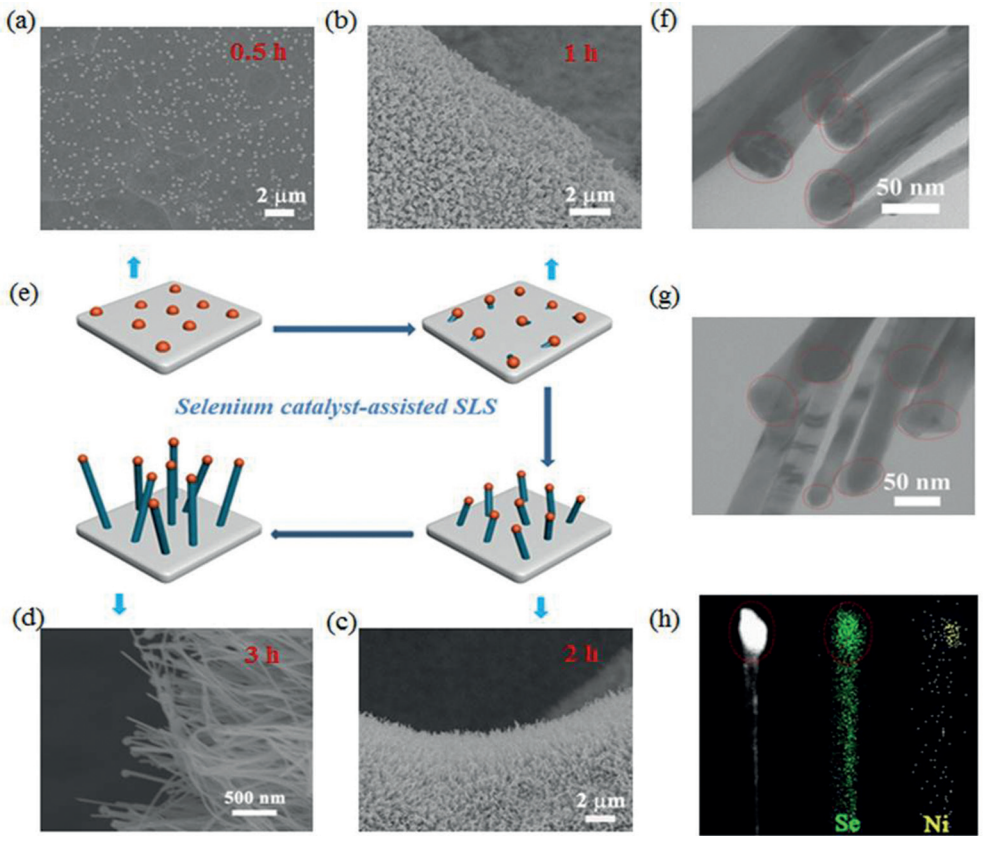

Figure 2. SEM image of the intermediate products at different reactions stages: a) 0.5 h, b) 1 h, c) 2 h, d) 3 h. e) Schematic illustration of the growth of NiSe nanowires by using a nonmetallic molecular crystal (Se) as catalyst. f,g) TEM images of the intermediate products. h) HAADF-STEM image of the intermediate product and corresponding elemental mapping.

Previous studies have demonstrated that Ni-based compounds are good candidates for OER catalysts because of their unique number of 3d electrons and special e_g orbitals.[19–21] Since a nanowire array grown directly on a conductive substrate could result in faster penetration of the electrolyte and diffusion of ionic species, it could also be expected that the NiSe nanowires/Ni foam would show a reasonable electrochemical performance for the electrocatalytic oxidation of water. To evaluate the electrocatalytic performance of the NiSe nanowires/Ni foam for the OER, the electrochemical measurements were carried out in an O_2-saturated alkaline solution of 1 M KOH. About 20 cycles were needed to activate the electrode before recording the cyclic voltammetry (CV) polarization curves of the NiSe/Ni foam. As a comparison, bare Ni foam and commercial Pt/C deposited on an Ni foam were also tested under the same conditions. Their CV curves were normalized by the geometric area of the Ni foam (Figure 3a). The broad redox

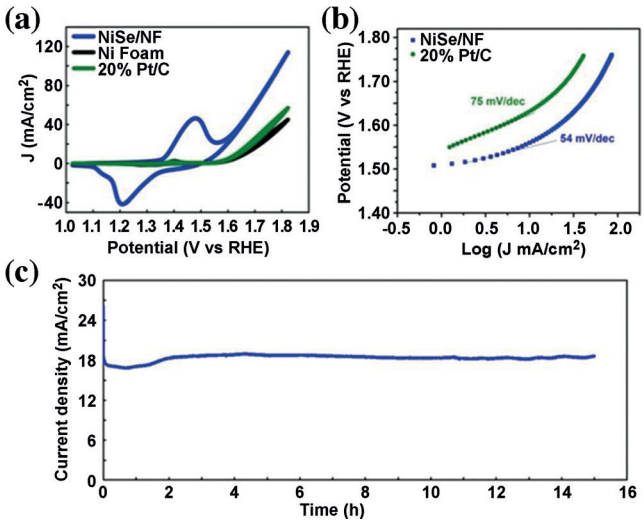

Figure 3. a) Cyclic voltammetry curves of the NiSe nanowires/Ni foam, Pt/C, and blank Ni foam (not iR-corrected). b) Tafel plots of the NiSe nanowires/Ni foam and Pt/C. Note: to avoid the interference of the oxidation peak in the NiSe nanowires/Ni foam, we used the cathodic sweep as the OER current for the Tafel plots of the NiSe nanowires/Ni foam. c) Chronopotentiometry of NiSe nanowires/Ni foam at an overpotential of 0.35 V. NF = Ni foam.

peaks located at 1.45 V versus the reversible hydrogen electrode (RHE) arise from the Ni^{2+}/Ni^{3+} couple. Apparently, the NiSe nanowire/Ni foam takes on a much earlier onset potential and also presents a higher current density under a certain applied voltage, compared with the bare Ni foam and commercial Pt/C. For example, at an overpotential of 0.4 V, the OER current density of the NiSe nanowire/Ni foam was 35 mA cm^{-2}, approximately 5- and 3.6-fold higher than that of the Ni foam and commercial Pt/C, respectively. Furthermore, we determined the Tafel slopes for the NiSe nanowire/Ni foam and Pt/C (Figure 3b). The Tafel slope of the NiSe nanowire/Ni foam is 54 mV dec^{-1}, smaller than that of Pt/C (75 mV dec^{-1}), which suggests that the OER rate for the NiSe nanowire/Ni foam is more rapid. It is well known that stability is a key parameter to evaluate electrocatalysts. Chronopotentiometry was performed to evaluate the stability of the NiSe nanowire/Ni foam in the OER. As shown in Figure 3c, the current density of the OER shows no significant degradation during 15 h of continuous operation, which suggests that the NiSe nanowire/Ni foam has excellent stability for the electrochemical oxidation of water. Thus, the NiSe nanowire/Ni foam with its high catalytic activity as well as excellent stability would be a strong candidate for future electrochemical oxidation reactions of water.

To gain insight into the electrocatalytic mechanism of the NiSe nanowires, we performed "post-morten" X-ray photoelectron spectroscopy (XPS) and XRD analyses of the NiSe nanowires/Ni foam after prolonged electrochemical tests. In Figure 4a, the two peaks located at 855.4 eV and 873.2 eV can

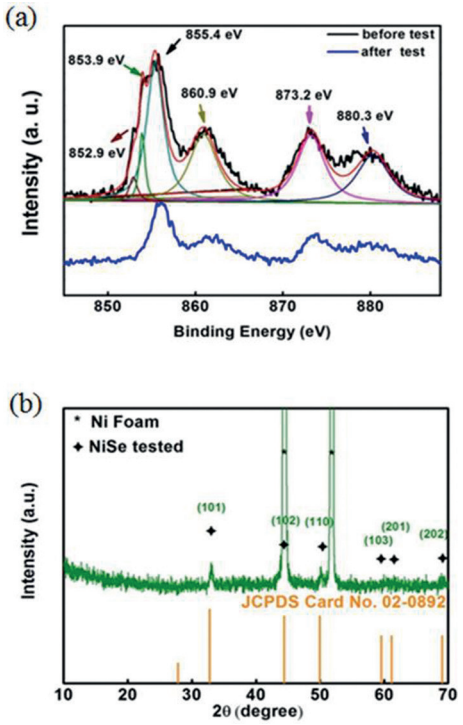

Figure 4. a) XPS spectrum of the initial NiSe nanowires/Ni foam and after 1000 OER cycles. b) XRD pattern of the NiSe nanowires/Ni foam after 1000 OER cycles.

be ascribed to Ni $2P_{3/2}$ and Ni $2P_{1/2}$, respectively. The peaks at 860.9 eV and 880.3 eV can be assigned to Ni satellite peaks of NiO, thus indicating the existence of surface oxidation on the NiSe nanowires.[22] Other peaks at 852.9 eV and 870.4 eV can be attributed to metallic Ni 2p originating from the Ni foam substrate.[23] Notably, the satellite peaks of NiO become relatively stronger after 1000 OER cycles, which demonstrates that the surface oxides become thicker. However, the nickel oxides/hydrated nickel oxides still couldn't be detected by XRD (Figure 4b), thereby indicating the major phase was always NiSe nanowires during the OER process. On the basis of the above analysis, it is reasonable to believe that NiSe nanowire cores inside with a very thin nickel oxide/hydroxide shell are the actual active sites during the OER process.

In summary, we have demonstrated that NiSe nanowire arrays can be synthesized by a SLS approach by using a nonmetal molecular crystal (selenium) as a catalyst. This synthesis brings SLS into the realm of conventional low-temperature solution synthesis. Studies of the time-dependent evolution of the morphology and elemental mapping have shown that selenium acts as the SLS catalyst. Intriguingly, the obtained array of NiSe nanowires was used as an electrocatalyst for the water oxidation, and exhibited a high activity and excellent stability. This study not only opens up a new approach to synthesize inorganic nanowire arrays, but also broadens our horizons to the SLS synthesis of inorganic nanowires with a nonmetal catalyst.

Acknowledgements

This work was financially supported by the National Basic Research Program of China (2015CB932302), Natural Science Foundation of China (no. 21222101, U1432133, 11132009, 21331005, 11321503, J1030412), Chinese Academy of Science (XDB01020300), the Fok Ying-Tong Education Foundation, China (grant no. 141042), the China Postdoctoral Science Foundation (No. 2015M580539)and the Fundamental Research Funds for the Central Universities (no. WK2060190027).

Keywords: electrochemistry · heterogeneous catalysis · nanostructures · oxidation · selenium

How to cite: *Angew. Chem. Int. Ed.* **2016**, *55*, 1710–1713
Angew. Chem. **2016**, *128*, 1742–1745

[1] H. Zhu, Y. Fu, F. Meng, X. Wu, Z. Gong, Q. Ding, M. V. Gustafsson, M. T. Trinh, S. Jin, X. Y. Zhu, *Nat. Mater.* **2015**, *14*, 636–642.
[2] Z. Liu, J. Xu, D. Chen, G. Shen, *Chem. Soc. Rev.* **2015**, *44*, 161–192.
[3] X. Wang, B. Liu, R. Liu, Q. Wang, X. Hou, D. Chen, R. Wang, G. Shen, *Angew. Chem. Int. Ed.* **2014**, *53*, 1849–1853; *Angew. Chem.* **2014**, *126*, 1880–1884.
[4] N. P. Dasgupta, J. Sun, C. Liu, S. Brittman, S. C. Andrews, J. Lim, H. Gao, R. Yan, P. Yang, *Adv. Mater.* **2014**, *26*, 2137–2184.
[5] J. Wallentin, N. Anttu, D. Asoli, M. Huffman, I. Åberg, M. H. Magnusson, G. Siefer, P. Fuss-Kailuweit, F. Dimroth, B. Witzigmann, H. Q. Xu, L. Samuelson, K. Deppert, M. T. Borgström, *Science* **2013**, *339*, 1057–1060.
[6] P. Jiang, Q. Liu, Y. Liang, J. Tian, A. M. Asiri, X. Sun, *Angew. Chem. Int. Ed.* **2014**, *53*, 12855–12859; *Angew. Chem.* **2014**, *126*, 13069–13073.
[7] X. Xia, C. Zhu, J. Luo, Z. Zeng, C. Guan, C. F. Ng, H. Zhang, H. J. Fan, *Small* **2014**, *10*, 766–773.
[8] T. Y. Ma, S. Dai, M. Jaroniec, S. Z. Qiao, *J. Am. Chem. Soc.* **2014**, *136*, 13925–13931.
[9] K. Wang, H. Wu, Y. Meng, Z. Wei, *Small* **2014**, *10*, 14–31.
[10] Y. Xia, P. Yang, Y. Sun, Y. Wu, B. Mayers, B. Gates, Y. Yin, F. Kim, H. Yan, *Adv. Mater.* **2003**, *15*, 353–389.
[11] R. Laocharoensuk, K. Palaniappan, N. A. Smith, R. M. Dickerson, D. J. Werder, J. K. Baldwin, J. A. Hollingsworth, *Nat. Nanotechnol.* **2013**, *8*, 660–666.
[12] F. Panciera, Y. C. Chou, M. C. Reuter, D. Zakharov, E. A. Stach, S. Hofmann, F. M. Ross, *Nat. Mater.* **2015**, *14*, 820–825.
[13] R. S. Wagner, W. C. Ellis, *Appl. Phys. Lett.* **1964**, *4*, 89–90.
[14] F. Wang, A. Dong, J. Sun, R. Tang, H. Yu, W. E. Buhro, *Inorg. Chem.* **2006**, *45*, 7511–7521.
[15] S. Jianwei, W. E. Buhro, *Angew. Chem. Int. Ed.* **2008**, *47*, 3215–3218; *Angew. Chem.* **2008**, *120*, 3259–3262.
[16] N. Kornienko, D. D. Whitmore, Y. Yu, S. R. Leone, P. Yang, *ACS Nano* **2015**, *9*, 3951–3960.
[17] X. Lu, K. J. Anderson, P. Boudjouk, B. A. Korgel, *Chem. Mater.* **2015**, *27*, 6053–6058.
[18] S. Liu, X. Guo, M. Li, W.-H. Zhang, X. Liu, C. Li, *Angew. Chem. Int. Ed.* **2011**, *50*, 12050–12053; *Angew. Chem.* **2011**, *123*, 12256–12259.
[19] K. Xu, P. Chen, X. Li, Y. Tong, H. Ding, X. Wu, W. Chu, Z. Peng, C. Wu, Y. Xie, *J. Am. Chem. Soc.* **2015**, *137*, 4119–4125.
[20] W. Zhou, X.-J. Wu, X. Cao, X. Huang, C. Tan, J. Tian, H. Liu, J. Wang, H. Zhang, *Energy Environ. Sci.* **2013**, *6*, 2921–2924.
[21] X. Long, J. Li, S. Xiao, K. Yan, Z. Wang, H. Chen, S. Yang, *Angew. Chem. Int. Ed.* **2014**, *53*, 7584–7588; *Angew. Chem.* **2014**, *126*, 7714–7718.
[22] P. Prieto, V. Nistor, K. Nouneh, M. Oyama, M. Abd-Lefdil, R. Díaz, *Appl. Surf. Sci.* **2012**, *258*, 8807–8813.
[23] G. K. Wertheim, S. Hüfner, *Phys. Rev. Lett.* **1972**, *28*, 1028–1031.

Received: September 17, 2015
Published online: December 22, 2015

